

Smart Electrical Infrastructure for AC-Fed Railways With Neutral Zones

Eduardo Pilo, *Member, IEEE*, Sudip K. Mazumder, *Senior Member, IEEE*, and Ignacio González-Franco

Abstract—This paper presents a proposal to modify power supply systems currently used in ac-fed railways with neutral zones (NZs), in order to allow power-flow routing. The proposed system complements the existing infrastructure with additional power-electronic devices connected in parallel to both sides of the NZs, allowing control of power flow through adjacent electrical sections. The description and control of such a modified railway system is outlined in this paper. In addition, a mixed-integer programming optimization problem is formulated, which minimizes the investment and the operation costs, while ensuring the power supply to the train traffic. This optimization model is used to allow a systematic evaluation of the benefits of implementing such a railway smart grid system. Finally, a section of the high-speed line between Madrid and Barcelona is used as a case study, and the advantages of the proposed system are quantified in two different scenarios.

Index Terms—Controllability, efficiency, energy management, management, optimization, planning, power system, railway, smart grid.

I. INTRODUCTION

ELECTRIFIED railways are normally considered one of the most energy-efficient modes of transport, particularly over economically viable operating distances. One of the key factors for this higher efficiency is the interconnections of the trains via the catenary (or active rails in some cases), which allow trains to perform regenerative braking. In other words, a train equipped with a regenerative braking device, while undergoing deceleration due to braking, is able to act like a generator by efficiently feeding part or all of its kinetic energy, in the form of electrical power, to the traction electrical grid. For that reason, in the last two decades, research has focused on increasing the efficacy of the onboard regenerative braking systems by 1) enhancing the efficiency and the flexibility of the onboard electronic converters [1]–[3]; 2) optimizing the operation, for instance, by designing the train schedules or the driving to maximize the energy recovery [4]; and 3) enhancing the ability of the infrastructure to deal with excesses of power,

for instance, by using energy-storage devices and reversible substations in dc systems.

The development of electrical smart grids is producing technologies that allow a rich interaction between the agents of the overall system (e.g., utilities, consumers, small generators, etc.) based on active management of the demand and the generation and active control of the electrical networks [5]–[7]. Although railway electrical grids are a particular case of electrical grid, some of their characteristics make them unique. First of all, the loads vary spatiotemporally because the locations of the trains and their power demands vary on almost on a continual basis. Furthermore, the number of loads is relatively small, although their load demand can be high. In addition, the loads are somewhat predictable because the nominal schedules of the trains are known in advance and a railway control center controls the movement of each train. Furthermore, from the point of view of the public grid, a fleet of moving trains can be considered to be a source of stored energy fed by the kinetic energy of the moving trains.

In three-phase power systems, power-flow routing has been traditionally performed by phase-shifting transformers, which are a special type of transformer, allowing to vary the phase shifting between the primary and the secondary side normally in a controlled way [8]. Since the late 1990s, the development of flexible alternating current transmission system devices has allowed different kinds of power-flow controls in ac transmission grids [9], normally relying on the notion of series/parallel compensation. More recently, similar concepts have been developed for distribution networks, particularly as the smart grid paradigm began to be adopted [10]–[12]. Finally, although direct conversion of the power (as opposed to series/parallel compensation schemes) is still problematic due to the large amount of power to be managed in distribution networks, it may be a feasible approach in the future.

This paper presents an enhancement for those railway power systems (RPSs) using segmented topologies. The proposed system allows an increased degree of controllability of the infrastructure, which enables, for instance, power routing.

In the field of railway electrification, RPSs are normally classified in two groups according to the characteristics of the voltage used in the power supply: low-frequency systems (which include dc, 16.7 Hz, 20 Hz, and 25 Hz) and industrial-frequency systems (50 Hz and 60 Hz). Although all these systems can use segmented topologies, it is in industrial-frequency systems where segmentation is commonly used [13].

This paper has five more sections. Section II describes the topology of the ac-fed RPSs with neutral zones (NZs) (often

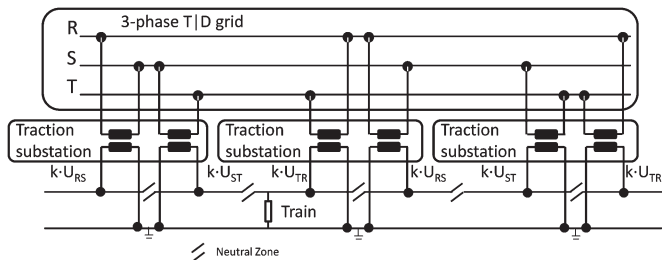
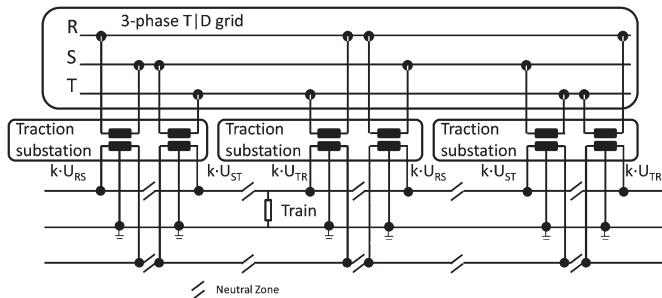
Manuscript received December 6, 2013; revised March 25, 2014; accepted June 20, 2014. The Associate Editor for this paper was H. Dong.

E. Pilo is with EPRail Research and Consulting, 28015 Madrid, Spain, and a Visiting Professor at the Department of Electrical and Computer Engineering, University of Illinois at Chicago, Chicago, IL 60607 USA (e-mail: eduardo.pilo@eprail.com).

S. K. Mazumder is with the Department of Electrical and Computer Engineering, University of Illinois at Chicago, Chicago, IL 60607 USA (e-mail: mazumder@uic.edu).

I. González-Franco is with Spanish Foundation of Railways, 28012 Madrid, Spain (e-mail: igonzalez@ffe.es).

Digital Object Identifier 10.1109/TITS.2014.2336535


 Fig. 1. Structure of a $1 \times$ RPS.

 Fig. 2. Structure of a $2 \times$ RPS.

referred to as industrial-frequency RPS). Section III describes the modification proposed in this paper and how it modifies the power distribution in a usual railway grid. Section IV proposes an optimization-based methodology to decide the dimensioning of the new elements to be installed. Its purpose is to evaluate the improvements that can be achieved with this technology and, therefore, its pertinence. This optimization methodology is then applied in Section V, using a case study based on a 550-km section of the Madrid–Barcelona high-speed line (HSL), and the results are analyzed. Finally, Section VI outlines the conclusions of this work.

II. POWER SUPPLY SYSTEMS USED IN RAILWAYS

Industrial-frequency RPSs are normally split into several feeding sections (FSs), each of which is fed from the three-phase public transmission or distribution grid (PTDG) through a single transformer located in a traction substation (TSS). The NZs are used to ensure electrical insulation between adjacent FSs.

Depending on the railways requirements, the FSs can be fed with the single-phase system with a neutral (referred to as $1 \times$) or the unbalanced two-phase autotransformer (AT)-based system with a neutral (referred to as $2 \times$), as illustrated in Figs. 1 and 2, respectively.

In the $2 \times$ system, although a two-phase system is set up, the loads are connected to only one phase (referred to as positive phase) and the neutral. The ATs are used to allow the flow of power from the other phase (referred to as the negative phase), which is unloaded [14].

In both Figs. 1 and 2, the symbols U_{RS} , U_{ST} , and U_{TR} refer to the voltages in the PTDG used to feed each transformer. Normally, the phases are rotated to reduce the unbalances caused by the railway grid in the PTDG.

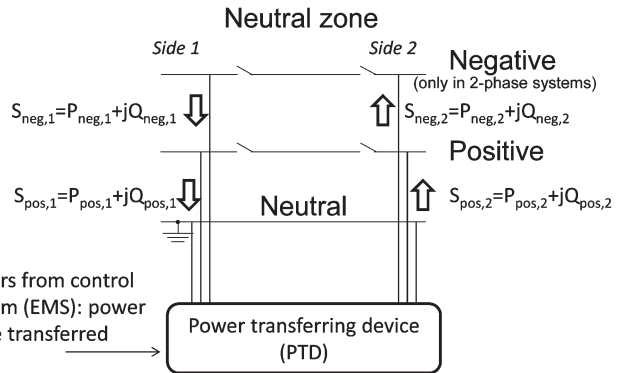


Fig. 3. Description of the PTDS.

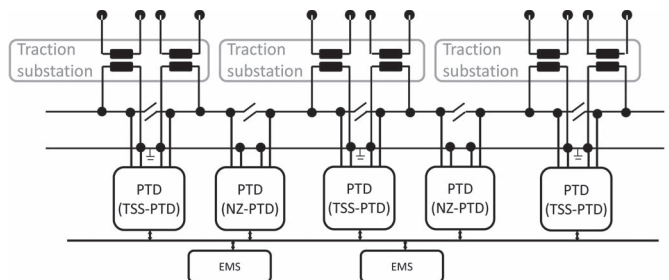


Fig. 4. Structure of the enhanced ac single-phase railway system.

III. PROPOSED ENHANCEMENT TO POWER SUPPLY SYSTEMS

A. Description of the Modified System

The proposed modification consists in the addition of a power-transferring device (PTD) connected in parallel to both sides of each NZ (see Fig. 3). A PTD has to be able to transfer, from one FS to the other, the active and reactive power specified by a control system, which is referred to as an energy management system (EMS), for the positive phase, as well as for the negative phase (in AT-based systems). In Fig. 3, symbols $S_{pos,i}$ and $S_{neg,i}$ refer to the apparent power transferred by the positive and negative phases, respectively, at the side i , with $i = \{1, 2\}$.

It should be noted that, although the rated voltages are the same in all the FSs, there are phase shifts between adjacent FSs due to the phase selection when connecting the transformers to the PTDG. In addition, in $2 \times$ systems, a phase shift exists between positive and negative voltages.

Fig. 4 shows the architecture of the enhanced $1 \times$ RPS, in which, for the sake of clarity, two EMSs have been considered. Fig. 5 shows the architecture of the enhanced ac $2 \times$ RPS with, for the sake of clarity, also two EMSs. The acronym TSS-PTD refers to the PTDs located in the NZ of the TSS. The acronym NZ-PTD refers to the PTDs located in the other NZs.

Although the EMS architecture details are beyond the scope of this paper, NZs are normally operated by a substation (TSS or NZ-specific substation, depending on the cases), where reliable communication channels are available, allowing a centralized as well as a distributed-control system for the modified system. While the centralized architecture enables the control system to perform a global optimization of the operation, particularly in terms of energy-management efficiency, the distributed control yields enhanced redundancy for the railway systems.

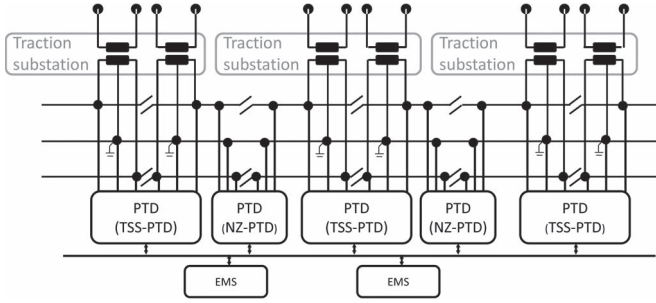


Fig. 5. Structure of the enhanced ac two-phase AT-based railways system.

B. Description of Operation of the Modified System

The power-balance expressions can be established for the general case (PTDs with star topology, with a higher number of terminals) as

$$\sum_{s=1}^{N_s} \sum_{p \in \{\text{pos, neg}\}} S_{p,s} = 0 \quad (1)$$

where N_s is the number of sides of the PTDs.

For the two-side PTDs represented in Fig. 3, $N_s = 2$ and (1) becomes

$$S_{\text{pos},1} - S_{\text{pos},2} + S_{\text{neg},1} - S_{\text{neg},2} = 0. \quad (2)$$

The power balance can be also expressed as a function of voltages and currents at the terminals of the PTDs, using

$$\sum_{s=1}^{N_s} \sum_{p \in \{\text{pos, neg}\}} (V_{p,s} \angle \theta_{p,s}) \cdot (I_{p,s} \angle \theta_{p,s} + \varphi_{p,s})^* \quad (3)$$

where $V_{p,s}$ and $I_{p,s}$ are the voltage and the input current modules, respectively, in the terminal (p, s) (side s and phase p of the PTD); $\theta_{p,s}$ is the angle of the voltage in the terminal (p, s) ; $\varphi_{p,s}$ is the angle between the voltage and the current in the terminal (p, s) ; symbol $*$ represents the conjugate operand.

If the angle $\theta_{p,s}$ is taken as the reference in each terminal, then (3) can be expressed as

$$\sum_{s=1}^{N_s} \sum_{p \in \{\text{pos, neg}\}} (V_{p,s} \angle 0) \cdot (I_{p,s} \angle \varphi_{p,s})^*. \quad (4)$$

Finally, if each phase is managed separately avoiding any power transfer between different phases, (4) becomes

$$\sum_{s=1}^{N_s} (V_{p,s} \angle 0) \cdot (I_{p,s} \angle \varphi_{p,s})^* = 0 \quad \text{for each phase } p. \quad (5)$$

If the voltages on both sides of a PTD are assumed to have the same amplitude, then (5) reduces to

$$\sum_{s=1}^{N_s} I_{p,s} = 0 \quad \text{for each phase } p \quad (6)$$

where $I_{p,s} = I_{p,s} \angle \varphi_{p,s}$.

Fig. 6 illustrates the way the currents in each of the phases are modified, by adding the PTDs to the infrastructure.

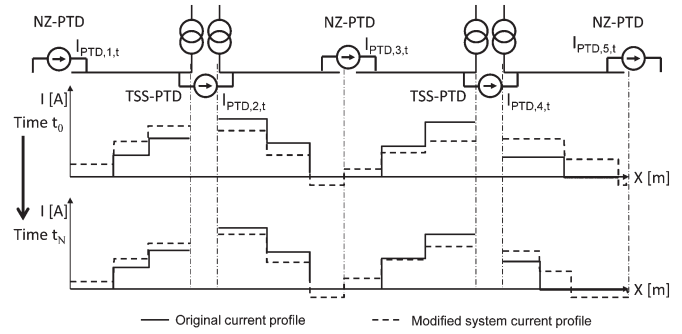


Fig. 6. Per-phase current distribution along the catenary.

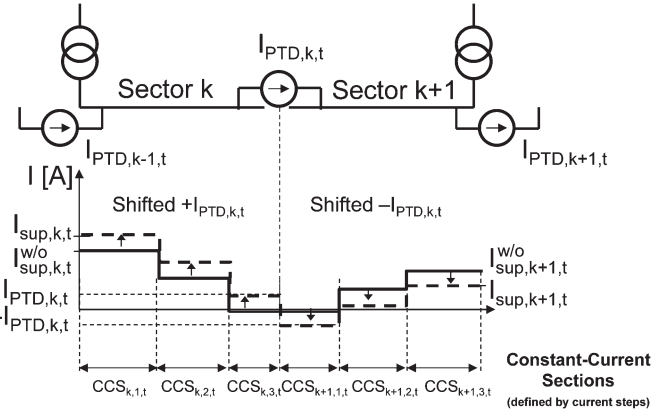


Fig. 7. Modification of the boundary condition for currents at the NZ.

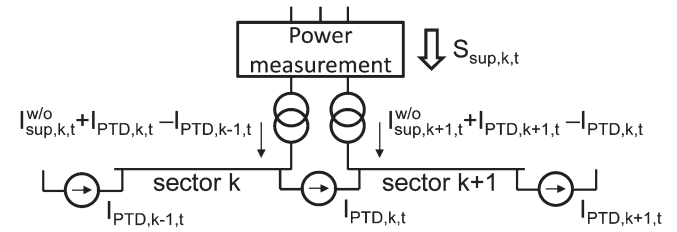


Fig. 8. Impact of the TSS-PTDs on the power supplied by a substation.

Fig. 7 shows how the NZ-PTD modifies the current steps in the catenary, increasing them in one side and decreasing them in the other. For a given phase, in the k th PTD, the injected currents at each time instant t have to be $I_{\text{PTD},k,t}$ on one side and $-I_{\text{PTD},k,t}$ on the other side.

Since the current supplied to the trains does not change if PTDs are added, the following expression can be established:

$$I_{\text{sup},k,t} = I_{\text{sup},k,t}^{\text{w/o}} + I_{\text{PTD},k,t} - I_{\text{PTD},k-1,t} \quad (7)$$

where $I_{\text{sup},k,t}^{\text{w/o}}$ is the current supplied by the transformer of sector k in the original system (without PTDs), $I_{\text{sup},k,t}$ is the current supplied by the transformer in the sector in the enhanced system (with PTDs), and $I_{\text{PTD},k,t}$ is the current transferred by the PTD k .

The power $S_{\text{sup},k,k+1,t}$ supplied by the substation containing transformers k and $k+1$ (see Fig. 8) can be derived from (7) as

$$S_{\text{sup},k,k+1,t} = V_{\text{sup}} (I_{\text{sup},k,t} + I_{\text{sup},k+1,t})^* \quad (8)$$

where V_{sup} is the supply voltage referred to the low-voltage side of the transformer.

TABLE I
 VARIABLES CONSIDERED IN THE OPTIMIZATION

| | |
|---------------|---|
| INV | Required investments [€] |
| OC | Operating manageable cost [€], as defined in (14) |
| $I_{rated,k}$ | Rated current of the PTD k [A] |
| $I_{PTD,k,t}$ | Current through PTD k at the instant t [A] |
| C_{lossC} | Cost of the energy losses in the catenary [€] |
| C_{lossX} | Cost of the energy losses in the transformers [€] |
| C_{pow} | Cost of the power capacity [€] |

If $\mathbf{I}_{sup,k,t}$ and $\mathbf{I}_{sup,k+1,t}$ are expressed as a function of the currents through the PTDs, the expression (8) becomes

$$\mathbf{S}_{sup,k,k+1,t} = V_{sup} \left(\mathbf{I}_{sup,k,t}^{w/o} + \mathbf{I}_{sup,k+1,t}^{w/o} + \mathbf{I}_{PTD,k+1,t} - \mathbf{I}_{PTD,k-1,t} \right)^* \quad (9)$$

Two important remarks can be formulated based on (9). The power $\mathbf{S}_{sup,k,k+1,t}$ supplied by the substation to the sectors k and $k+1$ does not depend on $\mathbf{I}_{PTD,k,t}$ (the current transferred by the TSS-PTD of the substation). Therefore, consequently, the real function of the TSS-PTDs has to be load balancing between the two transformers of the same substation.

IV. OPTIMAL RATING AND OPERATION

In order to evaluate the advantages of the system, an operation strategy of the infrastructure has been considered, consisting in minimizing the total cost of the electricity supply. Here, an optimization model is proposed to determine the most efficient operation of the PTDs and the optimal investments in PTDs to be done. This model takes into account the following: 1) the train power consumptions that have been previously obtained with a rail traffic simulator [15] and 2) the electrification to be upgraded (electrical description of the substations and catenaries) [16].

As indicated in (10), the cost of electricity C_{elec} is dependent on the usage of energy and the capacity of power allocated to a customer; that is

$$C_{elec} = C_{ene} \cdot E + C_{pc} \cdot P_{max} \quad (10)$$

where C_{ene} is the cost of the energy (in Euros per kilowatthour), E is the total energy consumption (in kilowatthours), C_{pc} is the cost of the allotted power capacity (in Euros per kilowatt), and P_{max} is the allotted power capacity (in kilowatts). Depending on the case, C_{elec} and C_{pc} may depend on the specific hour of the day.

The optimization determines the value of the variables listed in Table I, in order to minimize the economic impact of installing and operating PTDs, which include not only the required investments but also the savings in the electricity bill due to the proposed enhancement.

The objective function to be minimized is as follows:

$$INV + OC. \quad (11)$$

The investments include the cost of installing the PTDs in an existing infrastructure. Since voltage levels are known, the cost of each of the PTDs has been assumed to be proportional to the rated current of the PTDs, as follows:

$$INV = C_{dev,1} \sum_{k \in \text{PTD}} I_{rated,k} \quad (12)$$

 TABLE II
 SOS2 AUXILIARY VARIABLES

| | |
|---------------------|--|
| $I_{PTD,SOS,k,t,s}$ | Variable taking non-zero values only in the two adjacent values of s whose PTD currents are closer to $I_{PTD,k,t}$ (see Fig. 9), where s is the index of the considered step. |
| $I_{TR,SOS,k,t,s}$ | Variable taking non-zero values only in the two adjacent values of s whose currents are closer to the total current in transformer k (see Fig. 9). |

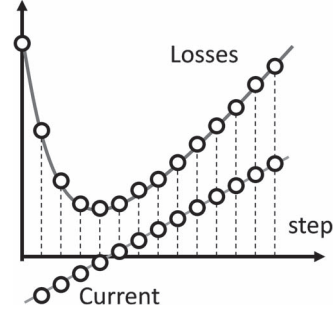


Fig. 9. Sampling of the losses and the currents for use with SOS2 variables.

where $C_{dev,1}$ is the cost per current unit of the PTD (in Euros, per ampere).

The current through the PTDs must be lower than its rated value to avoid a thermal destruction of the device. As the PTDs are bidirectional, the following constraint holds:

$$-I_{rated,k} \leq I_{PTD,k,t} \leq I_{rated,k} \quad \text{for each } t. \quad (13)$$

The operating manageable costs include the costs of the losses incurred in the transformers and the catenary, as well as the cost of the allotted power capacity, as

$$OC = C_{lossC} + C_{lossX} + C_{pow} \quad (14)$$

where $C_{ene} \cdot E = C_{lossC} + C_{lossX}$ and $C_{pc} \cdot P_{max} = C_{pow}$.

The cost of the losses in the transformer is as

$$C_{lossX} = C_{ene} R_x \delta_t \sum_t \sum_{k \in \text{TR}} \left(I_{sup,k,t}^{w/o} + I_{PTD,k+1,t} - I_{PTD,k-1,t} \right)^2 \quad (15)$$

where δ_t is the time step used in the traffic simulations, and the nonbold symbols I_x^y refer to the modules of the phasors \mathbf{I}_x^y for every index x and y (a power factor equal to one has been assumed).

The cost of the losses in the catenary is expressed by

$$C_{lossC} = C_{ene} \delta_t \sum_t \sum_{\substack{j \in \text{CCS}_{k,t} \\ k \text{ odd}}} R'_k D_{j,t} (I_{j,t} - I_{PTD,k,t})^2 \\ + C_{ene} \delta_t \sum_t \sum_{\substack{j \in \text{CCS}_{k,t} \\ k \text{ even}}} R'_k D_{j,t} (I_{j,t} - I_{PTD,k-1,t})^2 \quad (16)$$

where $\text{CCS}_{k,t}$ is the set of all the constant-current sections (CCSs) within the k th FS (see Fig. 7) at time step t , $I_{j,t}$ is the current in the j th CCS of a specific set $\text{CCS}_{k,t}$ at time step t , $D_{j,t}$ is the length of the j th CCS of $\text{CCS}_{k,t}$ at time step t , and R'_k is the resistance per length unit in the k th FS.

Simplified outline of the Madrid-Barcelona high speed line

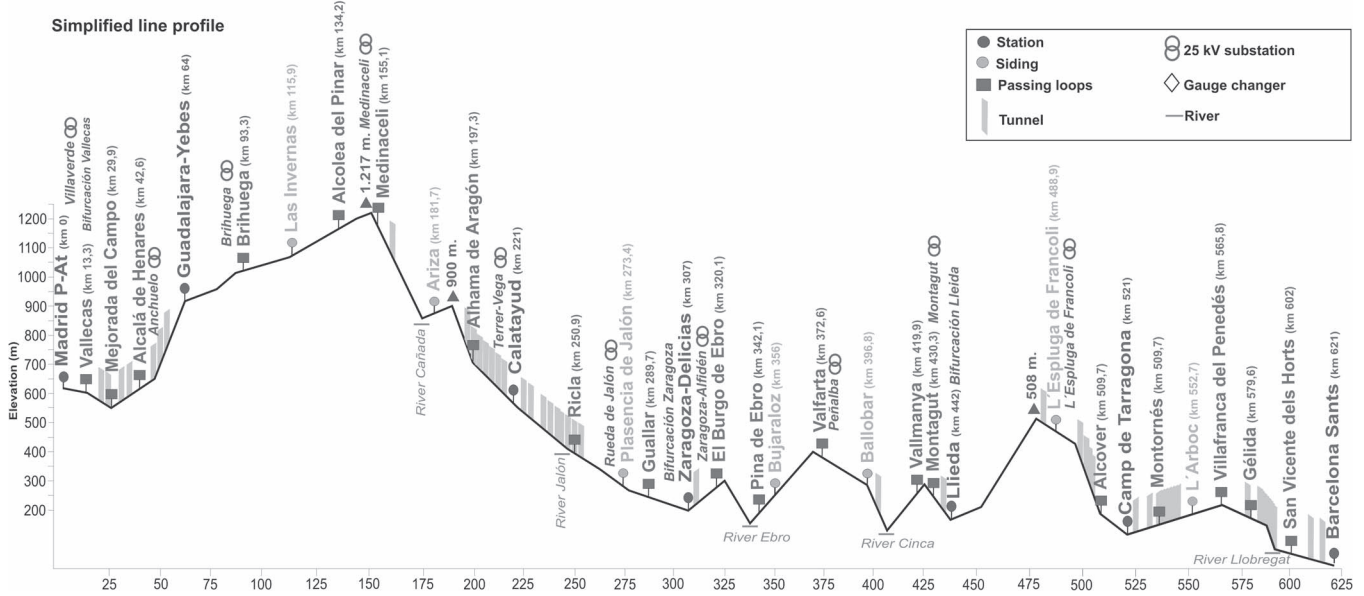


Fig. 10. Simplified outline of the HSL between Madrid and Barcelona.

Equation (16) can be rewritten as

$$\begin{aligned}
 C_{\text{loss}C} &= C_{\text{ene}} \delta_t \sum_t \sum_{\substack{j \in \text{CCS}_{k,t} \\ k \text{ odd}}} R'_k \\
 &\times (A_{k,t} + B_{k,t} I_{\text{PTD},k,t} + C_k I_{\text{PTD},k,t}^2) \\
 &+ C_{\text{ene}} \delta_t \sum_t \sum_{\substack{j \in \text{CCS}_{k,t} \\ k \text{ even}}} R'_k D_{j,t} \\
 &\times (A_{k,t} - B_{k,t} I_{\text{PTD},k-1,t} + C_k I_{\text{PTD},k-1,t}^2) \quad (17)
 \end{aligned}$$

where

$$\begin{cases}
 A_{k,t} = \sum_{j \in \text{CCS}_{k,t}} D_{j,t} I_{j,t}^2 \\
 B_{k,t} = 2 \sum_{j \in \text{CCS}_{k,t}} D_{j,t} I_{j,t} \\
 C_k = L_k
 \end{cases} \quad (18)$$

and L_k is the length of sector k .

As the restrictions (17) and (15) are quadratic with the set of variables $I_{\text{PTD},k,t}$, only nonlinear solvers can be used to solve the optimization problem. Hence, the problem is transformed into a mixed-integer programming (MIP) problem by performing a piecewise linearization of the losses, in which the auxiliary variables described in Table II are considered. To make the branch-and-bound process more efficient, special ordered sets type 2 (SOS2) have been used [17], [18].

The following additional restrictions are required for formulating the problem, in terms of the SOS2 variables

$$\sum_s I_{\text{PTD},\text{SOS},k,t,s} = 1 \quad (19)$$

$$\sum_s I_{\text{TR},\text{SOS},k,t,s} = 1. \quad (20)$$

In the optimization model, instead of using expressions (17) and (15) to calculate the power losses, $\text{LOSS}_{\text{CAT},k,t,s}$ and $\text{LOSS}_{\text{X},k,t,s}$ are defined with the precalculated values of the

losses at the catenary and the transformer in section k , at instant t , for the current step s (y -axis in Fig. 9), resulting in

$$C_{\text{loss}C} = C_{\text{ene}} \delta_t \sum_t \sum_k \sum_s I_{\text{PTD},\text{SOS},k,t,s} \cdot \text{LOSS}_{\text{CAT},k,t,s} \quad (21)$$

$$C_{\text{loss}X} = C_{\text{ene}} \delta_t \sum_t \sum_k \sum_s I_{\text{TR},\text{SOS},k,t,s} \cdot \text{LOSS}_{\text{X},k,t,s}. \quad (22)$$

Finally, the cost of the power capacity is given by

$$C_{\text{pow}} = C_{\text{pc},I} \sum_{k \text{ odd}} \max_t \left(I_{\text{sup},k,t}^{w/o} + I_{\text{PTD},k+1,t} - I_{\text{PTD},k-1,t} \right) \quad (23)$$

where $C_{\text{pc},I}$ is the cost of the allotted power capacity (in Euros, per ampere), assuming a given voltage in the power measuring point.

V. CASE STUDY

To evaluate the usefulness of the proposed system, a 549-km section of the HSL between Madrid and Barcelona is considered (from km 0 to km 549.153). In the study, the costs of the electrical power supply of the original and the optimized systems are compared.

Description of the case in Fig. 10 shows the simplified outline of the Madrid-Barcelona HSL. Except for the first 15 km, where the maximum speed is 250 km/h, trains can drive at 300 km/h for the rest of the studied section. There is an additional restriction in speed when arriving at Zaragoza (80 km/h at km 307) if the bypass is not taken.

Table III shows the sectors in this line section, the substations feeding them, their location, and the system (single-phase or two-phase). The location of the substations would also correspond to the location of the TSS-PTDs.

Table IV shows the location of the NZs of the line, which would also correspond to the location of NZ-PTDs.

TABLE III
SECTOR DESCRIPTION WITH SUBSTATIONS

| Sectors | Substation | | System |
|---------|----------------------------------|---------------|--------|
| | Transformer ID | Location [km] | |
| 1 | Villaverde (1x60MVA) | 0 (*) | 1-ph |
| 2, 3 | Anchuelo (2x60MVA) | 44.332 | 2-ph |
| 4, 5 | Brihuega-El Espino (2x60MVA) | 86.550 | 2-ph |
| 6, 7 | Medinaceli-Las Lastras (2x60MVA) | 152.417 | 2-ph |
| 8, 9 | Terrer-Vega (2x60MVA) | 214.819 | 2-ph |
| 10, 11 | Rueda de Jalón (2x60MVA) | 268.884 | 2-ph |
| 12, 13 | Zaragoza-Alfidén (2x60MVA) | 316.434 | 2-ph |
| 14, 15 | Peñalba (2x60MVA) | 377.587 | 2-ph |
| 15, 17 | Montagut (2x60MVA) | 430.466 | 2-ph |
| 18, 19 | L'Espluga (2x60MVA) | 490.795 | 2-ph |
| 20 | La Gornal (1x60MVA) | 549.253 | 2-ph |

(*)The location has been modified from its actual location, in order to match with the topology expected by the optimization model.

TABLE IV
NZ LOCATIONS

| Side sectors | Location [km] | Side sectors | Location [km] |
|--------------|---------------|--------------|---------------|
| 1, 2 | 20.999 | 11, 12 | 294.001 |
| 3, 4 | 67.693 | 13, 14 | 346.707 |
| 5, 6 | 112.174 | 15, 16 | 408.301 |
| 7, 8 | 188.963 | 17, 18 | 457.675 |
| 9, 10 | 241.250 | 19, 20 | 518.628 |

TABLE V
ELECTRICAL PARAMETERS OF THE LINE

| | |
|---|--------------------------------------|
| Catenary resistance [Ω /km] | |
| Sector 1 (1-phase) | 0.0661 |
| Sector 2 to 20 (2-phase) | 0.0226 |
| Transformer rated values | |
| Power [MVA] | 60 |
| Voltage at LV sides [kV] | 27.5 (1-ph), 27.5 / -27.5 kV (2-ph) |
| Ucc [%] | 15% (1-ph) |
| (X/R=10) | 12.5% (HV), 2.5% (LV Pos&Neg) (2-ph) |
| Transformer series resistance [Ω] at 25kV side | |
| Sector 1 (1-phase) | 0.15625 |
| Sector 2 to 20 (2-phase) | 0.15626 |

Table V shows the electrical parameters of the railway line, including the characteristics of the power transformers and the series line parameters of the catenaries. To transform two-phase systems to single-phase system, the equivalent model described in [19] has been used.

Siemens S-103 trains have been considered, with trains traveling every 10 min in each direction. Fig. 11 summarizes the characteristics of these trains.

Based on the aforementioned data, the power consumption of the trains in both directions has been obtained. Figs. 12 and 13 show the power consumption and the speed of the trains in the Madrid–Barcelona and Barcelona–Madrid journeys, respectively, sampled every 5 s. A power factor of 1 has been assumed.

To simplify the evaluation of the performance of the system, the periodic traffic mesh, with trains every 10 min, has been considered to operate 9 hours per day, 365 days a year. The number of operating hours may seem a bit low, but the frequency corresponds to a peak period.

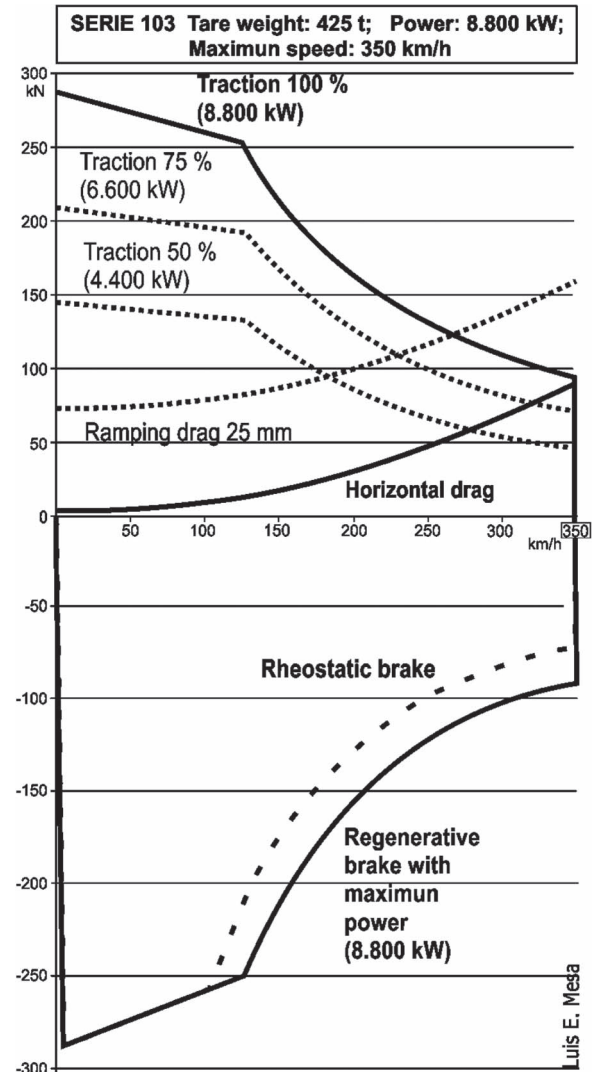


Fig. 11. Traction and braking curves of the S-103 trains.

For these average operating conditions, Table VI shows the estimated cost of the electricity, which has been considered.

A. Evaluation of the Enhanced System

In order to assess the advantages of the proposed system, its ability to control the power consumption of every substation and to reach an optimal operation is evaluated. However, the improvements are bounded by the rated currents of the PTDs, which depend on the investments: higher capacity PTDs may produce a more efficient operation, but are certainly more expensive items. As the proposed system is essentially a proof of concept, the prices of the PTDs are very difficult to estimate, particularly in the long term. For that reason, two scenarios have been studied.

- Scenario A: No cost has been considered for PTDs, i.e., $C_{dev,I} = 0 \text{ €/A}$, which leads to an optimal solution that only optimizes the operation, determining the rated currents of the PTDs that minimize the electricity costs. This case provides a good understanding of the best cost reduction that the system could reach if this technology would become massively adopted.

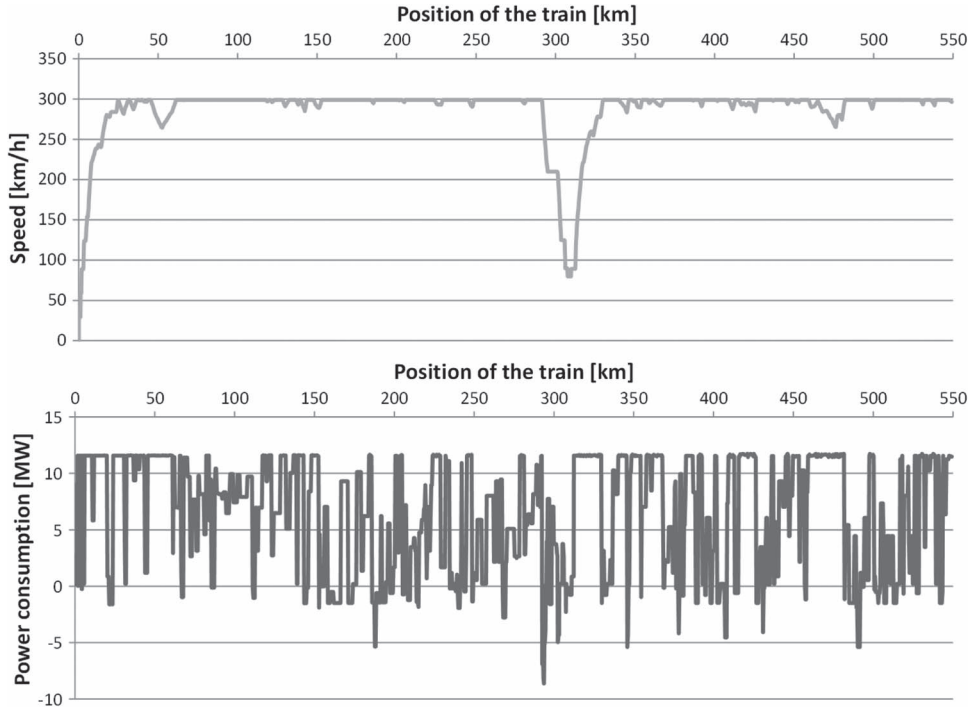


Fig. 12. Power consumption and speed, Madrid–Barcelona direction.

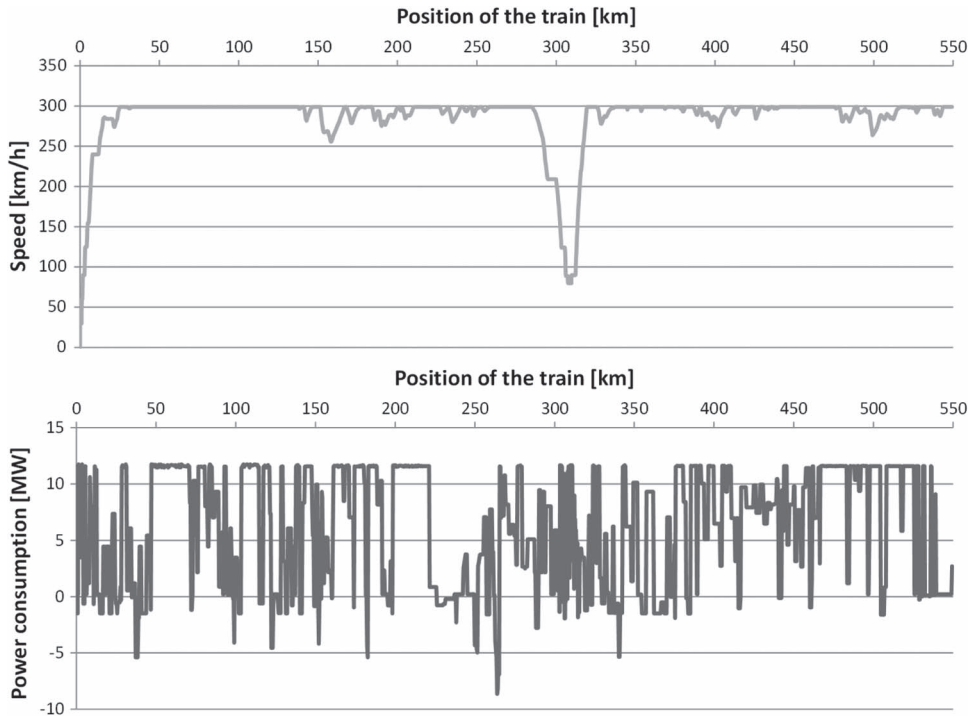


Fig. 13. Power consumption and speed, Barcelona–Madrid direction.

TABLE VI
COST OF THE ELECTRICITY (AVERAGED FOR > 145 kV, 2012, SPAIN)

| | |
|----------------|---|
| Power capacity | 23.92 €/kW/year 598 €/A/year at 25kV |
| Energy | 0.07 €/kWh |

sidered each year to be balanced with the electricity bill reductions, which makes $C_{dev,I} = 1025 \text{ €/A}$ (at 25 kV). In this case, the optimization will find a tradeoff between investments and energy savings, which gives a reference of the benefits of the proposed system for reducing the electricity costs.

- Scenario B: The cost of PTDs has been assumed to be 410 €/kVA. In addition, 10% of this cost will be con-

Fig. 14 and 15 compare the power supplied by every substation in scenarios A and B with the actual electrification,

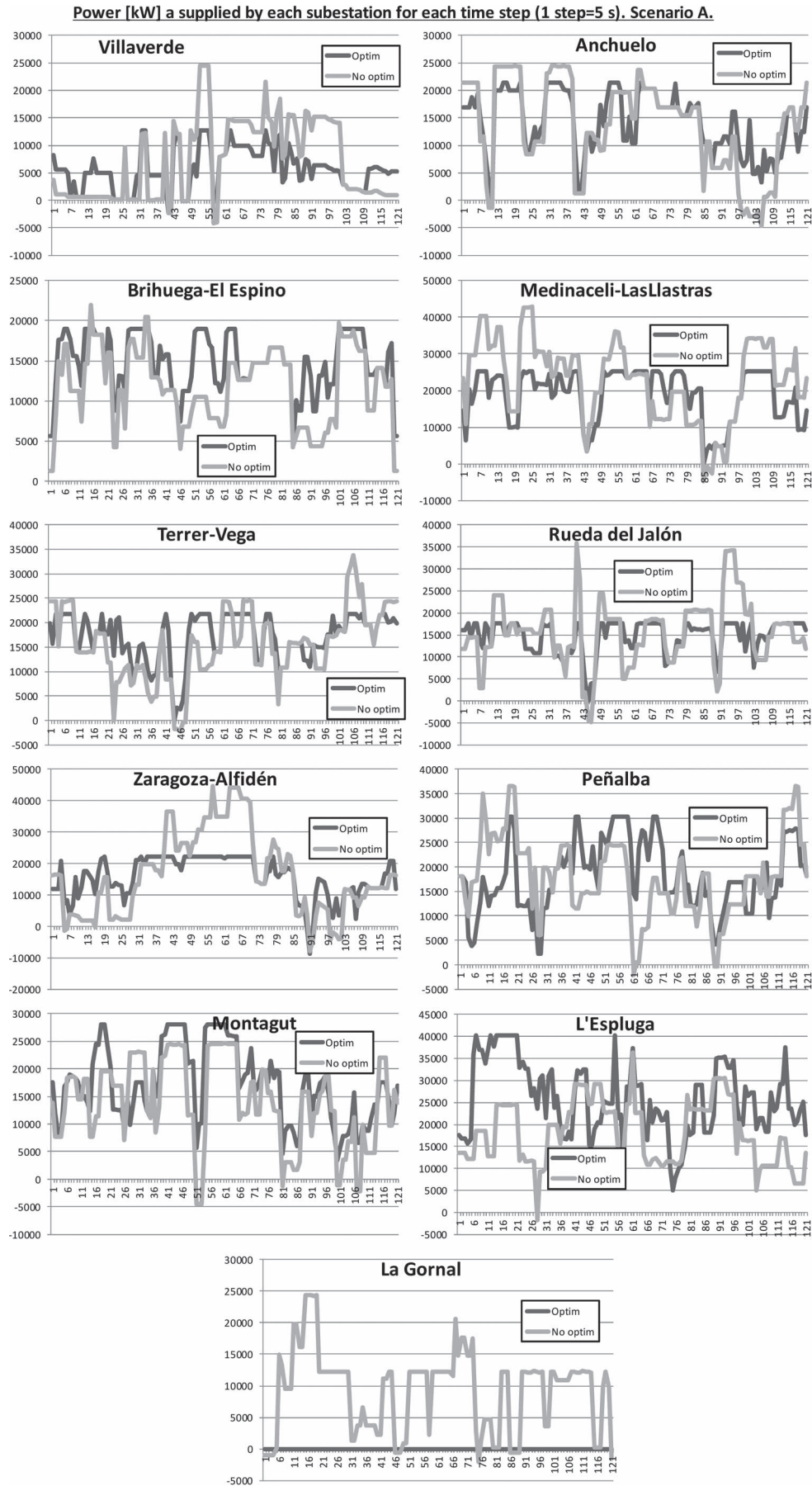


Fig. 14. Current supplied by the TSS for each instant. Reference versus Scenario A.

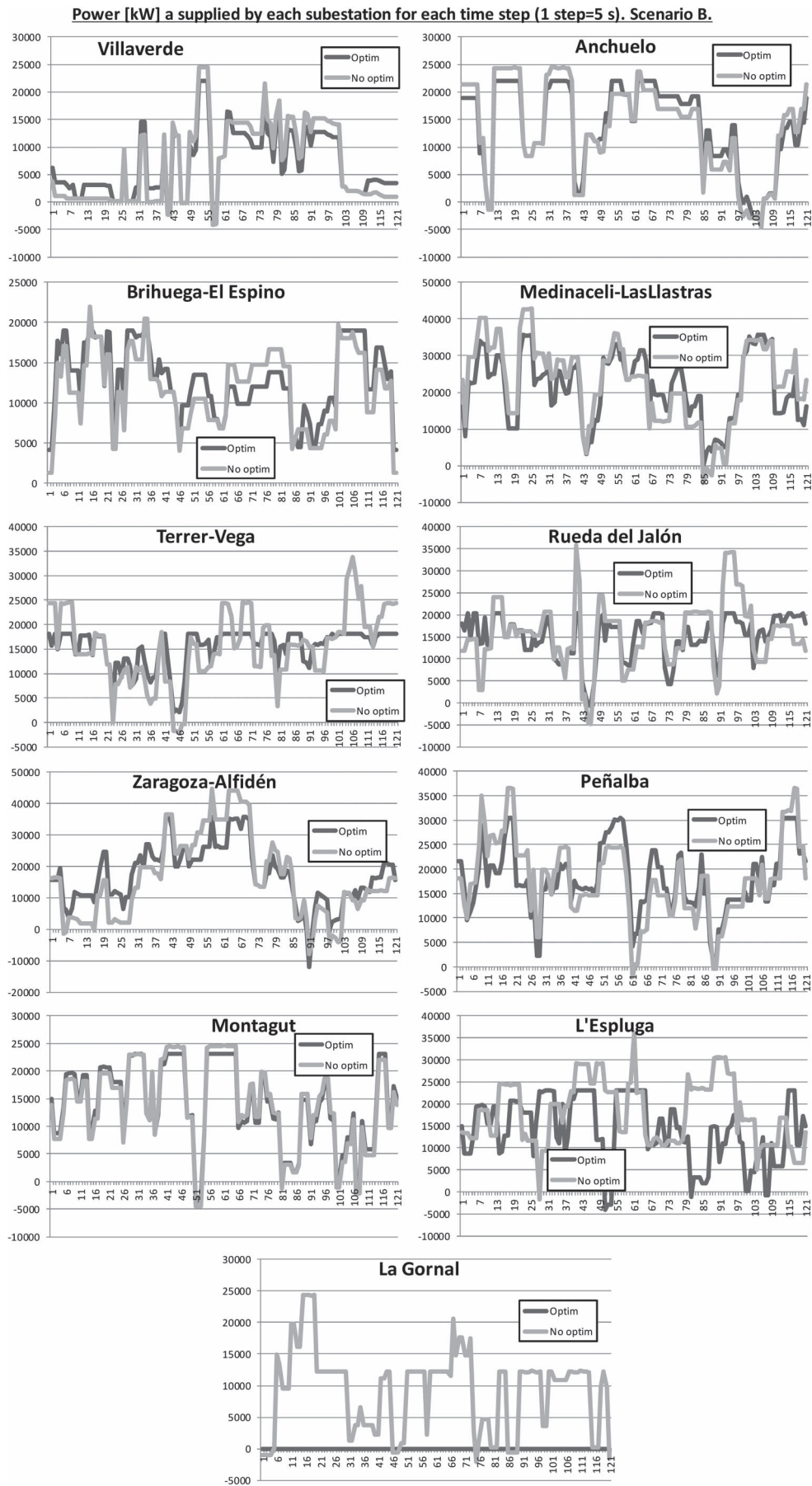


Fig. 15. Current supplied by TSS for each instant. Reference versus Scenario B.

TABLE VII
RATED CURRENTS OF THE PTDs

| Id | Between sectors | Type | Scenario A | Scenario B |
|----|-----------------|---------|-------------|-------------|
| | | | Rated I [A] | Rated I [A] |
| 1 | 1, 2 | NZ-PTD | 11837 | 2444 |
| 2 | 2, 3 | TSS-PTD | 15181 | 0 |
| 3 | 3, 4 | NZ-PTD | 10135 | 98 |
| 4 | 4, 5 | TSS-PTD | 9207 | 0 |
| 5 | 5, 6 | NZ-PTD | 9025 | 2861 |
| 6 | 6, 7 | TSS-PTD | 13200 | 0 |
| 7 | 7, 8 | NZ-PTD | 13200 | 4294 |
| 8 | 8, 9 | TSS-PTD | 13200 | 0 |
| 9 | 9, 10 | NZ-PTD | 13863 | 11337 |
| 10 | 10, 11 | TSS-PTD | 13200 | 0 |

| Id | Between sectors | Type | Scenario A | Scenario B |
|----|-----------------|---------|-------------|-------------|
| | | | Rated I [A] | Rated I [A] |
| 11 | 11, 12 | NZ-PTD | 16920 | 4110 |
| 12 | 12, 13 | TSS-PTD | 22000 | 0 |
| 13 | 13, 14 | NZ-PTD | 18865 | 4861 |
| 14 | 14, 15 | TSS-PTD | 17791 | 0 |
| 15 | 15, 16 | NZ-PTD | 8887 | 1313 |
| 16 | 16, 17 | TSS-PTD | 19795 | 0 |
| 17 | 17, 18 | NZ-PTD | 13200 | 234 |
| 18 | 18, 19 | TSS-PTD | 26798 | 0 |
| 19 | 19, 20 | NZ-PTD | 24380 | 24380 |

TABLE VIII
ECONOMIC ANALYSIS

| Per 1 year period | Reference system | Enhanced system | |
|--|------------------|-----------------|------------|
| | | Scenario A | Scenario B |
| Required peak capacity [MW] in substations | 350 | 238 | 275 |
| Variation (compared to ref.) | - | -32% | -21% |
| Cost of the power capacity [k€] | 8375 (94%) | 5696 | 6585 |
| Electrical losses [MWh] in catenary | 5293 | 5053 | 5572 |
| Variation (compared to ref.) | - | -5% | +5% |
| Cost of the electrical losses in catenary [k€] | 371 (4%) | 354 | 390 |
| Electrical losses [MWh] in transformers | 2737 | 1813 | 2620 |
| Variation (compared to ref.) | - | -34% | -4% |
| Cost of the electrical losses in transformers [M€] | 192 (2%) | 127 | 183 |
| Manageable electrical cost reduction [M€] | - | -2760 | -1778 |
| Variation (compared to ref.) | - | -31% | -20% |
| Cost of the PTDs [k€], per year | - | 0 | 2293 |

which is used as the reference. With the only exception of the substations “Montagut” and “L’Espluga” in scenario A, the maximum power peaks are significantly reduced. With the proposed system, all the power supply of the substation “La Gornal” is even effectively assumed by the other substations.

In addition, Table VII compares the rated values of the PTDs in both scenarios. In scenario A, as the cost of the PTDs is not considered in the objective function, the rated current of TSS-PTDs takes a nonzero value, in order to minimize losses in the transformers (as discussed previously, the function of the TSS-PTDs is mainly to balance the load supplied by the two transformers of the substation). In scenario B, the cost of the PTDs is largely higher compared to the cost of the transformer losses that can be saved by load balancing. Therefore, the optimization leads to not install TSS-PTDs at all.

Table VIII summarizes the enhancements due to adopting the proposed system in the analyzed line. The results obtained for the reference case shows that 94% of the manageable

cost of the electricity corresponds to the power capacity term, while the losses represent 4% (in the catenary) and 2% (in the transformers). The manageable cost of the electricity includes the cost of the power capacity and the cost of the losses in the catenary and the transformers, but excludes the cost of the energy consumed by trains (which is assumed not to be controlled by the infrastructure).

In scenario A, where PTDs can be rated to obtain the best improvements in the system regardless of their cost, the enhanced system would be able to cut down 32% of the power capacity costs and, very similarly, the losses. In this specific case, this would be an upper bound of the enhancement that the system could reach.

In scenario B, where real prices and a chargeoff of ten years have been considered, improvements are lower than in scenario A. However, a reduction of 20% in the manageable costs is reached, mainly due to the savings in the power capacity term (-21%). To achieve this, the system is able to route the electrical power from different substations to the sectors where it is required. In exchange, the currents have to cross longer distances, and the electrical losses rise up (+5%). The losses in the transformer are, however, reduced (-4%).

VI. CONCLUSION

This paper has presented a system to improve the ac railway power supply systems, which have NZs. The system allows an improved degree of controllability of the infrastructure, which allows for instance power routing in traction electrical grids. The proposed system could be an important milestone in the railway smart grid roadmap.

The proposed system would be able to route the electrical power routing, making possible new ways of operation of railway systems more reliable and cost efficient.

As an example of such intelligent operation of the RPS, a strategy focused on the minimization of the manageable costs of the power supply (including costs of the power capacity and losses) has been considered in a study case, which corresponds to a 550-km long section of the Madrid-Barcelona HSL. The system would be able to reduce up to 31% of these manageable costs of the electricity.

REFERENCES

- [1] J. O. Estima and A. J. Marques Cardoso, "Efficiency analysis of drive train topologies applied to electric/hybrid vehicles," *IEEE Trans. Veh. Technol.*, vol. 61, no. 3, pp. 1021–1031, Mar. 2012.
- [2] M. Chymera, A. C. Renfrew, M. Barnes, and J. Holden, "Simplified power converter for integrated traction energy storage," *IEEE Trans. Veh. Technol.*, vol. 60, no. 4, pp. 1374–1383, May 2011.
- [3] P. Drabek, Z. Peroutka, M. Pittermann, and M. Cédil, "New configuration of traction converter with medium-frequency transformer using matrix converters," *IEEE Trans. Ind. Electron.*, vol. 58, no. 11, pp. 5041–5048, Nov. 2011.
- [4] M. Peña-Alcaraz, A. Fernández, A. P. Cucala, A. Ramos, and R. R. Pecharrmán, "Optimal underground timetable design based on power flow for maximizing the use of regenerative-braking energy," *Proc. Inst. Mech. Eng. F, J. Rail Rapid Transit*, vol. 226, no. 4, pp. 397–408, Jun. 2012.
- [5] H. Hayashiya *et al.*, "Cost impacts of high efficiency power supply technologies in railway power supply—Traction and station," in *Proc. 15th Int. EPE/PEMC*, 2012, pp. LS3e.4-1–LS3e.4-6.
- [6] Y. Watanabe *et al.*, "Examination on application of a smart grid technology to stations," in *Proc. 15th Int. EPE/PEMC*, 2012, pp. DS2d.11-1–DS2d.11-5.
- [7] H. Hayashiya *et al.*, "Necessity and possibility of smart grid technology application on railway power supply system," in *Proc. 14th EPE Conf. Appl.*, 2011, pp. 1–10.
- [8] J. Verboomen, D. Van Hertem, P. H. Schavemaker, W. L. Kling, and R. Belmans, "Phase shifting transformers: Principles and applications," in *Proc. Int. Conf. Future Power Syst.*, 2005, pp. 1–6.
- [9] M. Noroozian, L. Angquist, M. Ghandhari, and G. Andersson, "Use of UPFC for optimal power flow control," *IEEE Trans. Power Del.*, vol. 12, no. 4, pp. 1629–1634, Oct. 1997.
- [10] J. B. Hamelink, P. H. Nguyen, W. L. Kling, P. F. Ribeiro, and R. J. W. De Groot, "Routing power flows in distribution networks using locally controlled power electronics," in *Proc. 47th Int. UPEC*, 2012, pp. 1–6.
- [11] P. H. Nguyen, W. L. Kling, and P. F. Ribeiro, "Smart power router: A flexible agent-based converter interface in active distribution networks," *IEEE Trans. Smart Grid*, vol. 2, no. 3, pp. 487–495, Sep. 2011.
- [12] P. H. Nguyen, W. L. Kling, and P. F. Ribeiro, "Agent-based power routing in active distribution networks," in *Proc. 2nd IEEE PES Int. Conf. Exhib. ISGT Europe*, 2011, pp. 1–6.
- [13] L. Abrahamsson, T. Schütte, and S. Östlund, "Use of converters for feeding of AC railways for all frequencies," *Energy Sustainable Develop.*, vol. 16, no. 3, pp. 368–378, Sep. 2012.
- [14] E. Pilo, L. Rouco, and A. Fernández, "A reduced representation of 2/spl times/25 kV electrical systems for high-speed railways," in *Proc. IEEE/ASME Joint Rail Conf.*, Chicago, IL, USA, 2003, pp. 199–205.
- [15] P. Lukaszewicz, "Energy consumption, running time for trains: Modelling of running resistance and driver behaviour based on full scale testing," Ph.D. dissertation, Dept. Veh. Eng., Royal Inst. Technol. (KTH), Stockholm, Sweden, 2001.
- [16] E. Pilo, L. Rouco, A. Fernández, and A. Hernández-Velilla, "A simulation tool for the design of the electrical supply system of high-speed railway lines," in *Proc. IEEE PES Summer Meet.*, Seattle, WA, USA, 2000, pp. 1053–1058.
- [17] A. Brooke and R. E. Rosenthal, *GAMS Development*. Washington, DC, USA: GAMS, 2003.
- [18] E. Beale and J. Forrest, "Global optimization using special ordered sets," *Math. Programm.*, vol. 10, no. 1, pp. 52–69, 1976.
- [19] E. Pilo, L. Rouco, A. Fernandez, and L. Abrahamsson, "A monovoltage equivalent model of bi-voltage autotransformer-based electrical systems in railways," *IEEE Trans. Power Del.*, vol. 27, no. 2, pp. 699–708, Apr. 2012.



Eduardo Pilo (M'00) received the M.Sc. and Ph.D. degrees from Comillas Pontifical University, Madrid, Spain, in 1997 and 2003, respectively.

From 2003 to 2010 he was a Researcher with the Institute for Research in Technology (IIT), School of Engineering (ICAI), Comillas Pontifical University, working both in the Railways Group (ASF) and in the Power System Modeling Group (MAC). In this period, as the technician responsible for the research projects related with traction power systems, he has participated in 39 projects sponsored by public and private institutions. Since 2003 he has been a Lecturer of several degree, master, and doctorate courses related with power systems and railways. Since 2010 he has been the Chief Executive Officer of EPRail Research and Consulting, Madrid (<http://www.eprail.com>), which is a company focused on power systems and railways. He is currently a Visiting Professor at University of Illinois at Chicago, Chicago, IL, USA.



Sudip K. Mazumder (SM'03) received the M.S. degree in electrical power engineering from Rensselaer Polytechnic Institute, Troy, NY, USA, in 1993 and the Ph.D. degree in electrical and computer engineering from Virginia Polytechnic Institute and State University, Blacksburg, VA, USA, in 2001.

He is a Professor with the Department of Electrical and Computer Engineering, University of Illinois at Chicago (UIC), Chicago, IL, USA, where he is the Director of the Laboratory for Energy and Switching-Electronics Systems. He has over 22 years of professional experience and has held research and development positions in leading industrial organizations, and has served as a Technical Consultant for several industries. He has published over 150 refereed papers in journals and conferences and has published one book and six book chapters. Twenty-four of his journal papers are published in IEEE Transactions, with a current impact factor greater than 4. He has presented 49 invited/plenary/keynote presentations and currently holds six issued and three pending patents.

Dr. Mazumder is the President of NextWatt LLC, a small business organization that he started in 2008. Since joining UIC, he has received close to 40 sponsored projects by the National Science Foundation, the Department of Energy, Office Naval Research, Consulting Engineers Council, the Environmental Protection Agency, the Air Force Research Laboratory, National Aeronautics and Space Administration, the Advanced Research Projects Agency-Energy, the Naval Sea Systems Command (NAVSEA), and multiple leading industries.



Ignacio González-Franco received the degree in industrial engineering from University of Vigo, Vigo, Spain, and the M.Sc. degree in railway engineering from Comillas Pontifical University, Madrid, Spain.

He is with the Spanish Foundation of Railways (FFE), Madrid, where he is the Coordinator of the Energy and Emissions with the Railways Research Group and the Technical and Economic Transport Operations Research Group. He has experience in the railways sector, having taken part in different research projects. He is currently writing his doctoral thesis in the optimization of transport infrastructures.